International Offshore Wind Technical Conference – IOWTC 2021
February 16-17, 2021, Virtual Conference
IOWTC 2021-3503

A REDUCED-ORDER MATHEMATICAL MODEL FOR THE CURRENT-INDUCED MOTION OF A FLOATING OFFSHORE WIND TURBINE

Éverton L. de Oliveira
Celso P. Pesce
Bruno Mendes
Renato M. M. Orsino
Guilherme R. Franzini

Offshore Mechanics Laboratory
Polytechnic School of University of São Paulo

IOWTC
International Offshore Wind Technical Conference

Presentation Outline

1) Introduction

2) Motivation and Objectives

3) The Reduced-Order Mathematical Model

4) A Case Study

5) Conclusions and Further Works

6) References

1) Introduction

2) Motivation and Objectives

3) The Reduced-Order Mathematical Model

4) A Case Study

5) Conclusions and Further Works

6) References

○ Introduction

- Floating platforms, originally employed as solutions for the offshore oil and gas sector, have been used recently in the offshore wind energy industry to give support to wind turbines in mid and relatively deep waters;
- In the case of floating platforms with circular columns, Vortex-Induced Motion (VIM) can be an important phenomenon;
- Computational Fluid Dynamics (CFD) modeling might be used as a prediction tool for VIM. However, the high computational time usually impairs this approach, at least during design stages;
- Alternatively, phenomenological models, based on non-linear oscillators, such as on van der Pol equations are proper to wake dynamics modeling.

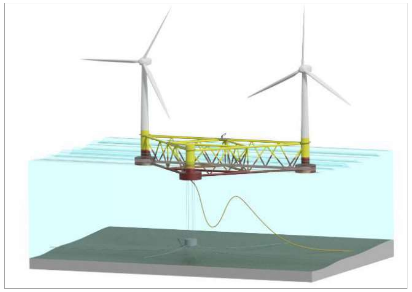

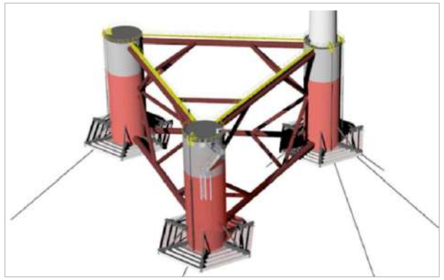

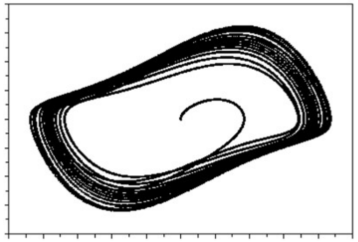

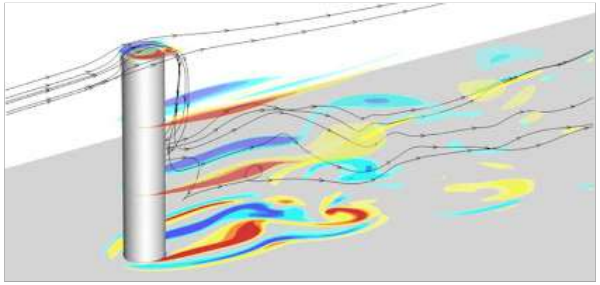

- Introduction
  - **Early studies**

Authors	Description
Hartlen & Currie (1970)	One of the pioneering studies, proposing the use of the Rayleigh oscillator in order to model the lift coefficient. The coupling with the cylinder dynamics was made through velocity.
Facchinetti et al. (2003)	Concluded that the interaction between wake and cylinder dynamics equations might be modeled as dominated by inertial terms, proposing then a coupling in terms of acceleration.
Ogink & Metrikine (2010)	Relaxed an important hypothesis of Facchinetti et al's model, namely, the linearization of the instantaneous relative velocity of the cylinder with respect to the flow, modifying the coupling parameters, according to the experimentally observed vortex emission regime.
Franzini & Bunzel (2018)	Extended the approach by Ogink and Metrikine to two degrees of freedom (2-dof), allowing both crosswise and in-line oscillations. A second van der Pol oscillator, vibrating twice as fast as the crosswise one, was introduced.

○ Motivation

- The present work was motivated by the recent experimental results of Gonçalves et al. (2019), on the existence of VIM on a small-scale multicolumn FOWT-OC-4 model;
- If proved to be relevant in full scale, VIM might consist in a significant factor to the operation of wind turbines;
- CFD might be computationally demanding;
- The intent henceforth is to verify whether reduced order models based on wake oscillators could be successfully applied to multicolumn platforms;
- In the present work, using the formalism of Analytical Mechanics and based on wake oscillators phenomenological approach, a reduced-order mathematical model (ROM) is derived to assess the motion on the horizontal plane;
- The FOWT-OC-4 Phase II is used as case study and numerical results are confronted with the experimental data by Gonçalves et al. (2019);
- A full-scale FOWT with pontoons is used as a second case study.

The Reduced Order Mathematical Model

Equations of motion on the horizontal plane

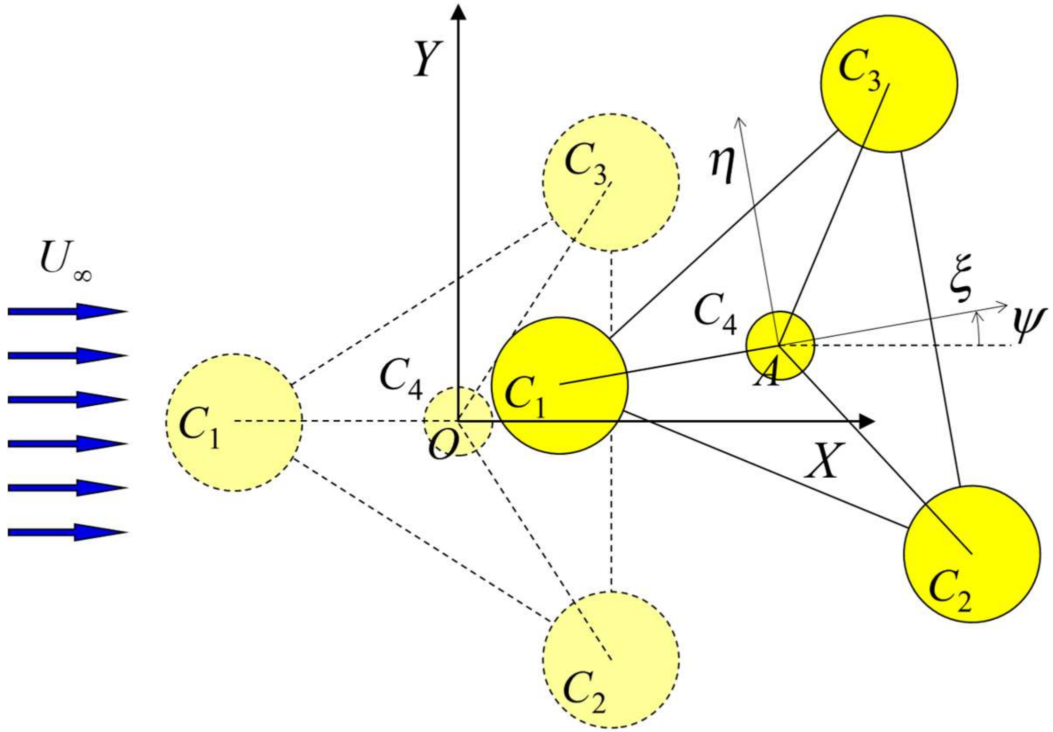

Coordinates and general definitions. At origin, platform is shown at 0 degrees current heading.

- Generalized coordinates (rigid-body motions):

$$\mathbf{q} = [x \quad y \quad \psi]^T,$$

- Lagrange's equations of motion:

$$\frac{d}{dt}\left(\frac{\partial T}{\partial \dot{\mathbf{q}}}\right) - \frac{\partial T}{\partial \mathbf{q}} = \mathbf{Q}^m + \mathbf{Q}^v,$$

- Kinetic energy (including the added mass effects):

$$T = \frac{1}{2}\dot{\mathbf{q}}^T \mathbf{M}\dot{\mathbf{q}}; \quad \mathbf{M} = \mathbf{M}_p + \mathbf{M}_a; \quad \mathbf{M}_a = \mathbf{B}\hat{\mathbf{M}}_a\mathbf{B}^T,$$

- Equations of motion:

$$\mathbf{M}\ddot{\mathbf{q}} + \mathbf{Q}^I = \mathbf{Q}^m + \mathbf{Q}^v,$$

- Nonlinear inertial terms
- Generalized restoring mooring forces
- Generalized hydrodynamic forces (vortex shedding)

Pesce et al. (2018)

○ The Reduced Order Mathematical Model

○ Phenomenological model and hydrodynamic forces

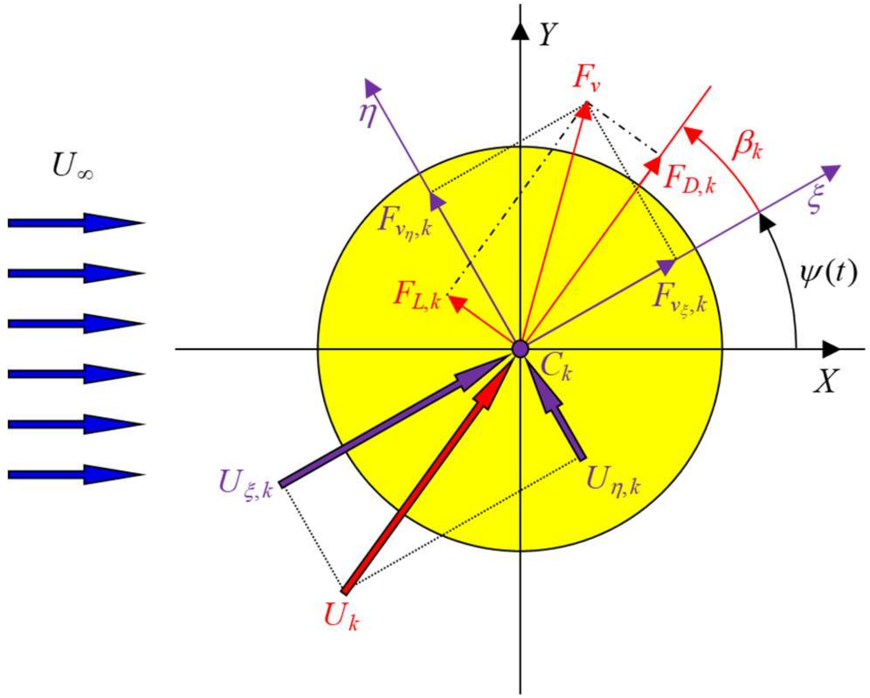

Forces diagram for the k-th column. Cylinder moving left and down.

Hydrodynamic interferences are not considered

- Body-fixed components of the hydrodynamic forces:

$$F_{v_{\xi,k}} = \frac{1}{2}\rho D_k H_k C_{\xi,k} U_\infty^2; \quad F_{v_{\eta,k}} = \frac{1}{2}\rho D_k H_k C_{\eta,k} U_\infty^2,$$

$$U_{\xi,k} = U_{\infty,\xi} - v_{C_{k,\xi}}; \quad U_{\eta,k} = U_{\infty,\eta} - v_{C_{k,\eta}}; \quad U_k = \sqrt{U_{\xi,k}^2 + U_{\eta,k}^2},$$

- Body-fixed hydrodynamic coefficients:

$$C_{\xi,k} = (C_{D,k} U_{\xi,k} - C_{L,k} U_{\eta,k}) \frac{U_k}{U_\infty^2},$$

$$C_{\eta,k} = (C_{D,k} U_{\eta,k} + C_{L,k} U_{\xi,k}) \frac{U_k}{U_\infty^2},$$

- Velocity of the k-th column center:

$$\mathbf{v}_{C_k} = \mathbf{v}_A + \boldsymbol{\omega}_p \times \mathbf{r}_{C_k | A},$$

- Generalized viscous hydrodynamic forces:

$$Q_j^v = \sum_{k=1}^{N_c} \mathbf{F}_{v,k} \cdot \frac{\partial \mathbf{v}_{C_k}}{\partial \dot{q}_j}; \quad j = 1,2,3.$$

The Reduced Order Mathematical Model

Phenomenological model and hydrodynamic forces

- Two forced van der Pol oscillators for each column, aligned with the body-frame directions

$$\ddot{w}_{\xi,k} + \varepsilon_\xi \omega_{s,k} (w_{\xi,k}^2 - 1)\dot{w}_{\xi,k} + 4\omega_{s,k}^2 w_{\xi,k} = \frac{A_\xi}{D_k} a_{\xi,k},$$

$$\ddot{w}_{\eta,k} + \varepsilon_\eta \omega_{s,k} (w_{\eta,k}^2 - 1)\dot{w}_{\eta,k} + \omega_{s,k}^2 w_{\eta,k} = \frac{A_\eta}{D_k} a_{\eta,k},$$

$$\omega_{s,k} = 2\pi S_{t,k} \left(U_k / D_k\right),$$

- Lift and drag coefficients as functions of the wake variables:

$$C_{L,k} = \frac{C_{L0}}{2} w_{\eta,k}; \quad C_{D,k} = C_{D0}(1 + K w_{\eta,k}^2) + \frac{C_{D0}^f}{2} w_{\xi,k},$$

- Coupling with body-fixed hydrodynamic coefficients:

$$C_{\xi,k} = (C_{D,k} U_{\xi,k} - C_{L,k} U_{\eta,k}) \frac{U_k}{U_\infty^2}; \quad C_{\eta,k} = (C_{D,k} U_{\eta,k} + C_{L,k} U_{\xi,k}) \frac{U_k}{U_\infty^2}.$$

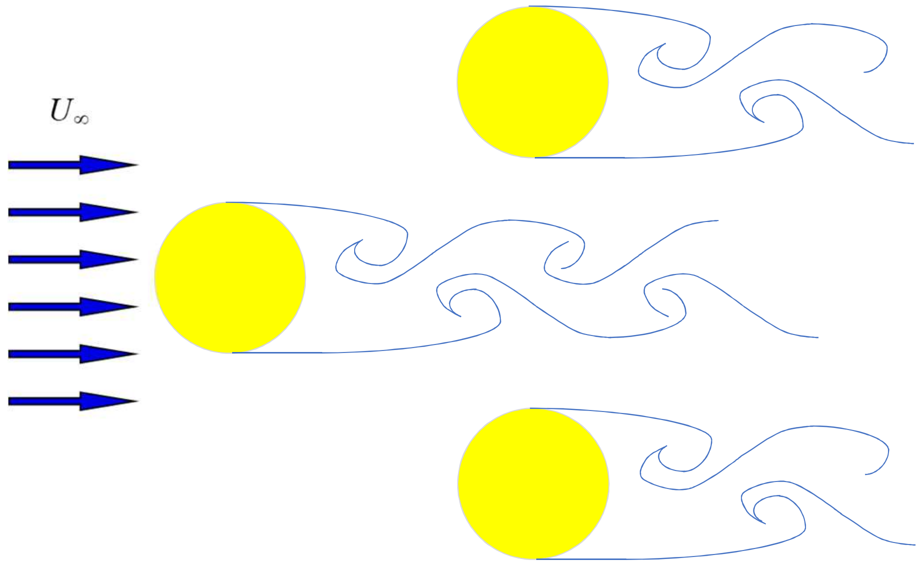

Vortex wake shed from each cylindrical column. No wake interference is considered.

The Reduced Order Mathematical Model

The coupled fluid-structure interaction ROM

- A 11-dof reduced-order model is obtained (3 rigid body dof + 2 x 4 columns wake oscillators):

$$\tilde{\mathbf{M}}\ddot{\tilde{\mathbf{q}}} = \tilde{\mathbf{Q}}_c + \tilde{\mathbf{Q}}_{nc},$$

$$\tilde{\mathbf{M}} = \begin{bmatrix} \mathbf{M} & \mathbf{0} \\ \mathbf{A}_w & \mathbf{1} \end{bmatrix}; \ \tilde{\mathbf{q}} = \begin{bmatrix} \mathbf{q} \\ \mathbf{w} \end{bmatrix},$$

$$\tilde{\mathbf{Q}}_c = \begin{bmatrix} \mathbf{Q}^m - \mathbf{Q}^I \\ \mathbf{Q}_w^r \end{bmatrix}; \ \tilde{\mathbf{Q}}_{nc} = \begin{bmatrix} \mathbf{Q}^v \\ \mathbf{Q}_w^v \end{bmatrix},$$

- Generalized coordinate vector, $\tilde{\mathbf{q}}$;
- Augmented inertia matrix, $\widetilde{\mathbf{M}}$;
- Generalized conservative forces and nonlinear inertia terms, $\tilde{\mathbf{Q}}_C$;
- Non-conservative term, $\tilde{\mathbf{Q}}_{nc}$.

$$\mathbf{A}_w = \begin{bmatrix} -\frac{A_\xi}{D_1}\frac{\partial a_{\xi,1}}{\partial \ddot{q}_1} & -\frac{A_\xi}{D_1}\frac{\partial a_{\xi,1}}{\partial \ddot{q}_2} & -\frac{A_\xi}{D_1}\frac{\partial a_{\xi,1}}{\partial \ddot{q}_3} \\ -\frac{A_\eta}{D_1}\frac{\partial a_{\eta,1}}{\partial \ddot{q}_1} & -\frac{A_\eta}{D_1}\frac{\partial a_{\eta,1}}{\partial \ddot{q}_2} & -\frac{A_\eta}{D_1}\frac{\partial a_{\eta,1}}{\partial \ddot{q}_3} \\ \vdots & \vdots & \vdots \\ -\frac{A_\xi}{D_{N_c}}\frac{\partial a_{\xi,N_c}}{\partial \ddot{q}_1} & -\frac{A_\xi}{D_{N_c}}\frac{\partial a_{\xi,N_c}}{\partial \ddot{q}_2} & -\frac{A_\xi}{D_{N_c}}\frac{\partial a_{\xi,N_c}}{\partial \ddot{q}_3} \\ -\frac{A_\eta}{D_{N_c}}\frac{\partial a_{\eta,N_c}}{\partial \ddot{q}_1} & -\frac{A_\eta}{D_{N_c}}\frac{\partial a_{\eta,N_c}}{\partial \ddot{q}_2} & -\frac{A_\eta}{D_{N_c}}\frac{\partial a_{\eta,N_c}}{\partial \ddot{q}_3} \end{bmatrix}; \ \mathbf{Q}_w^r = \begin{bmatrix} -4\omega_{s,1}^2 w_{\xi,1} \\ -\omega_{s,1}^2 w_{\eta,1} \\ \vdots \\ -4\omega_{s,N_c}^2 w_{\xi,N_c} \\ -\omega_{s,N_c}^2 w_{\eta,N_c} \end{bmatrix}; \ \mathbf{Q}_w^v = \begin{bmatrix} -\varepsilon_\xi \omega_{s,1}(w_{\xi,1}^2 - 1)\dot{w}_{\xi,1} \\ -\varepsilon_\eta \omega_{s,1}(w_{\eta,1}^2 - 1)\dot{w}_{\eta,1} \\ \vdots \\ -\varepsilon_\xi \omega_{s,N_c}(w_{\xi,N_c}^2 - 1)\dot{w}_{\xi,N_c} \\ -\varepsilon_\eta \omega_{s,N_c}(w_{\eta,N_c}^2 - 1)\dot{w}_{\eta,N_c} \end{bmatrix}.$$

- Experimental Study of a FOWT (Gonçalves et al., IOWTC 2019)
  - **FOWT-OC-4 Phase II**

- Reduced scale model (1:72.72):

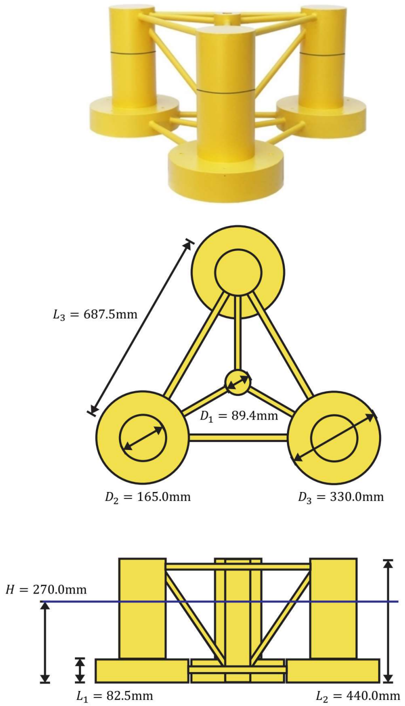

$$L/D = H/D = 1.67$$

- Schematic diagram of the experiment:

0 (°), 90 (°), 180 (°)

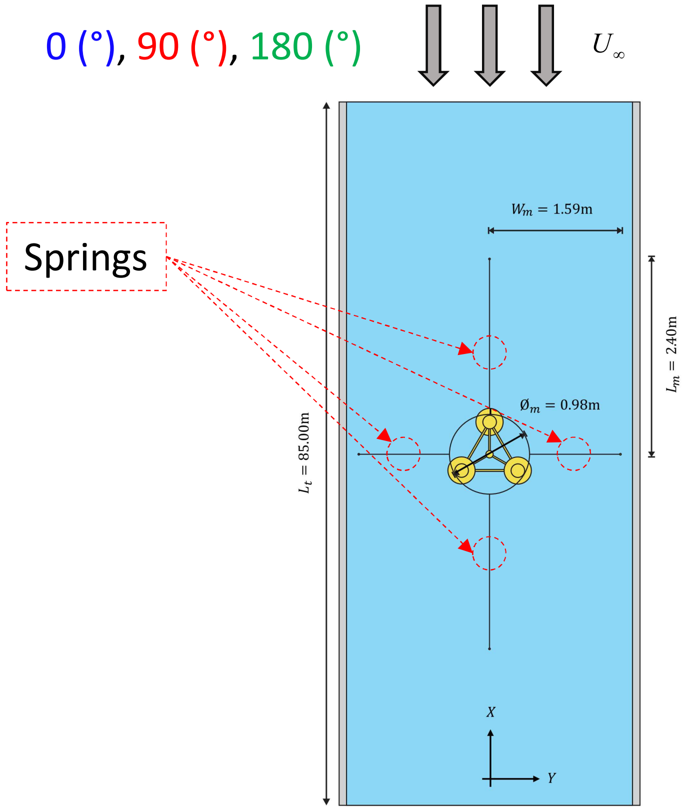

- Experimental Study of a FOWT
  - **FOWT-OC-4 Phase II**

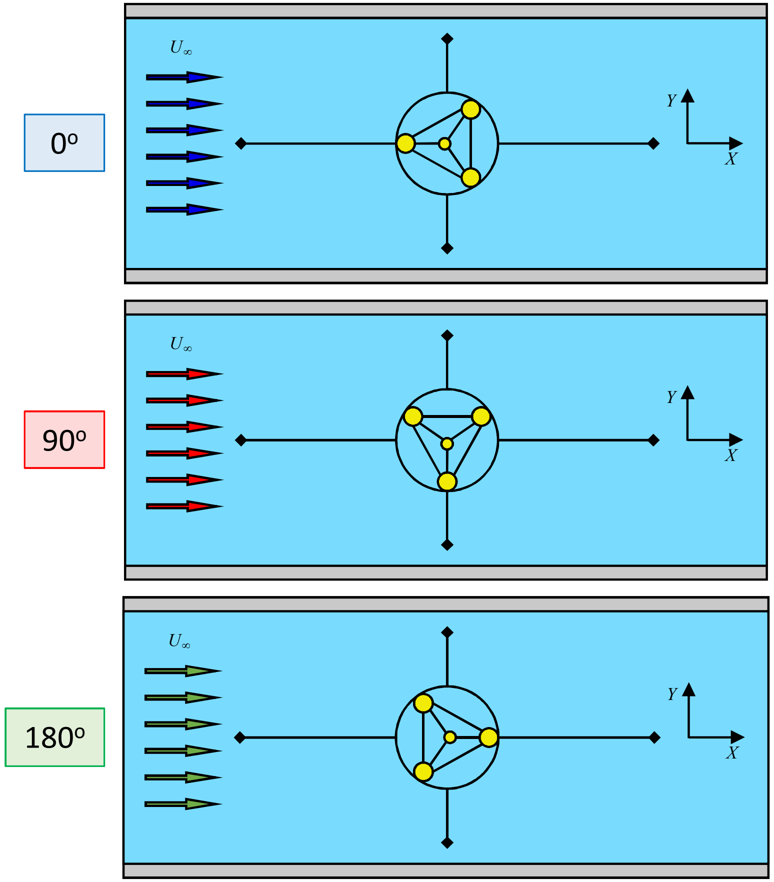

The platform is rotated relative to the support ring to set up the different heading angles.

- Numerical Simulations
  - **Simulations' setup**

    - Simulations were carried out at least for 30 reduced velocities ($3 < V_R < 24$ and $8{,}000 < Re < 70{,}000$) for each incidence angle;
    - The simulations were performed in a MATLAB® environment, numerically integrating the coupled equations in the state space form;
    - A fixed time step of 0.1 seconds was used, applying the 4th order Runge-Kutta algorithm;
    - The results obtained are:
      1) Natural periods at the trivial equilibrium position (origin, $\boldsymbol{q} = \boldsymbol{0}$);
      2) FOWT's trajectories on the horizontal plane;
      3) Dimensionless motion amplitudes and oscillation frequencies.

Numerical Simulations

Parameters

Table 1. OC4 scaled model parameters.

Parameters	Values
Draught, H (m)	0.275
Arc radius, R (m)	0.490
Columns centers' radius, r (m)	0.397
Diameters, $\{D_1, D_2, D_3, D_4\}$ (m)	{0.165, 0.165, 0.165, 0.090}
Platform's mass matrix, $\mathbf{M}_p$ (kg, kg, kgm²)	diag{36.70, 36.70, 4.00}
Added mass tensor, $\hat{\mathbf{M}}_a$ (kg, kg, kgm²)	diag{21.72, 22.13, 4.39}
Density of water, ρ (kg/m³)	1000

Table 2. Mooring system parameters.

Parameters	Values
Towing car dimensions, $\{W_m, L_m, \Phi_m\}$ (m)	{1.59, 2.40, 0.98}
Natural lengths $\{l_{n_1}, l_{n_2}, l_{n_3}, l_{n_4}\}$ (m)	{0.80, 0.425, 0.80, 0.425}
Spring constants $\{k_1, k_2, k_3, k_4\}$ (N/m)	{7.46, 9.42, 7.46, 9.42}

Table 3. Wake-oscillators parameters.

Parameters	Values
$\{A_\xi, A_\eta\}$	{12, 6}
$\{\varepsilon_\xi, \varepsilon_\eta\}$	{0.30, 0.15}
$\{C_{D0}, C_{L0}, C^f_{D0}, K\}$	{0.70, 0.30, 0.10, 0.05}
Strouhal numbers for each column, $\{S_{t_1}, S_{t_2}, S_{t_3}, S_{t_4}\}$	{0.145, 0.145, 0.145, 0.150}

Table 4. Mass and stiffness matrices at the trivial equilibrium position.

Incidence	0°, 180°	90°
Mass matrix, $\mathbf{M}$ (kg, kg, kgm²)	diag{58.42, 58.83, 8.39}	diag{58.83, 58.42, 8.39}
Mooring stiffness matrix, $\mathbf{K}$ (N/m, N/m, Nm)	diag{26.48, 27.46, 19.22}	diag{26.48, 27.46, 19.22}

Table 5. Natural periods at the trivial equilibrium position.

	Experiment		ROM	
Incidence	0°, 180°	90°	0°, 180°	90°
DOF	T_n (s)	T_n (s)	T_n (s)	T_n (s)
X	9.40	9.40	9.33	9.36
Y	9.60	9.70	9.20	9.16
ψ	4.20	4.20	4.15	4.15

- Parameters
- Results

Results

Trajectories of the FOWT's center on the horizontal plane

0°

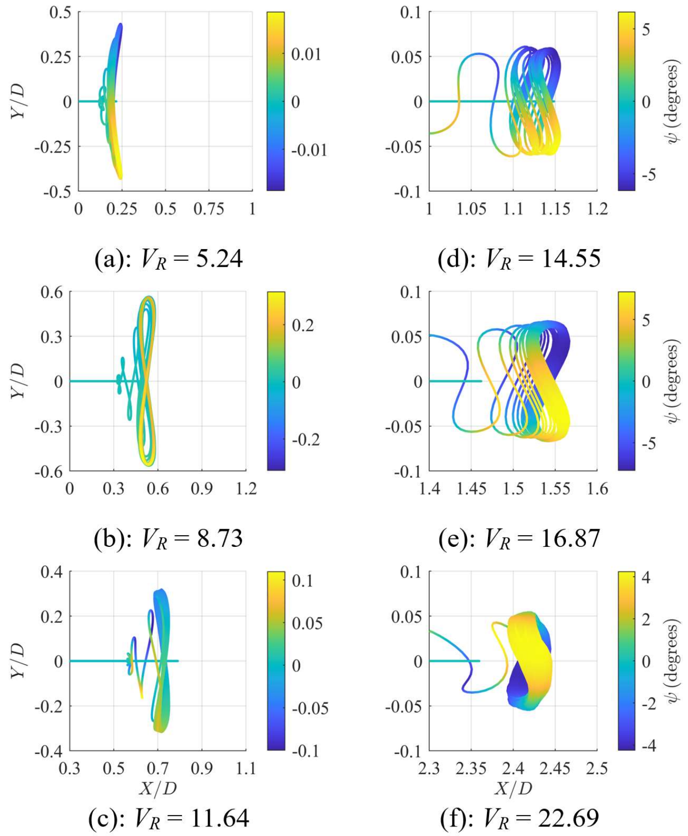

X is the current direction, in-line; Y is the direction transversal to it, cross. Yaw scaled as in the colored bar.

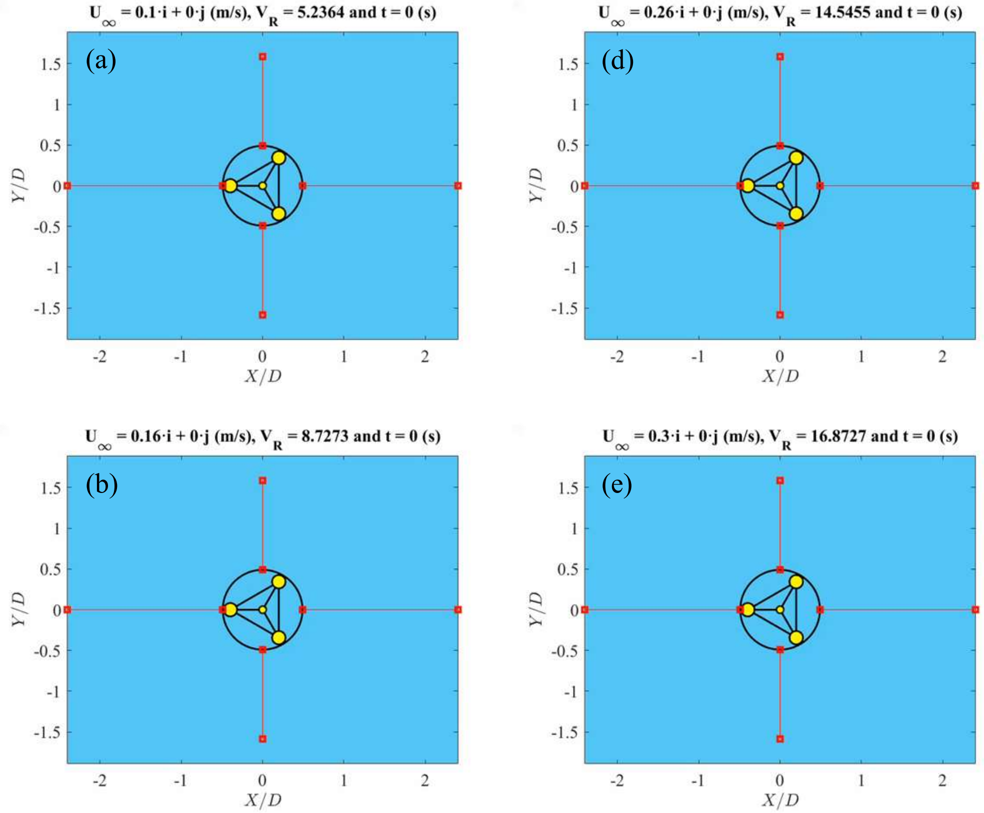

Animation of the FOWT's motion at the corresponding reduced velocities. Platform drawing in augmented scale (6x).

Results

Trajectories of the FOWT’s center on the horizontal plane

90°

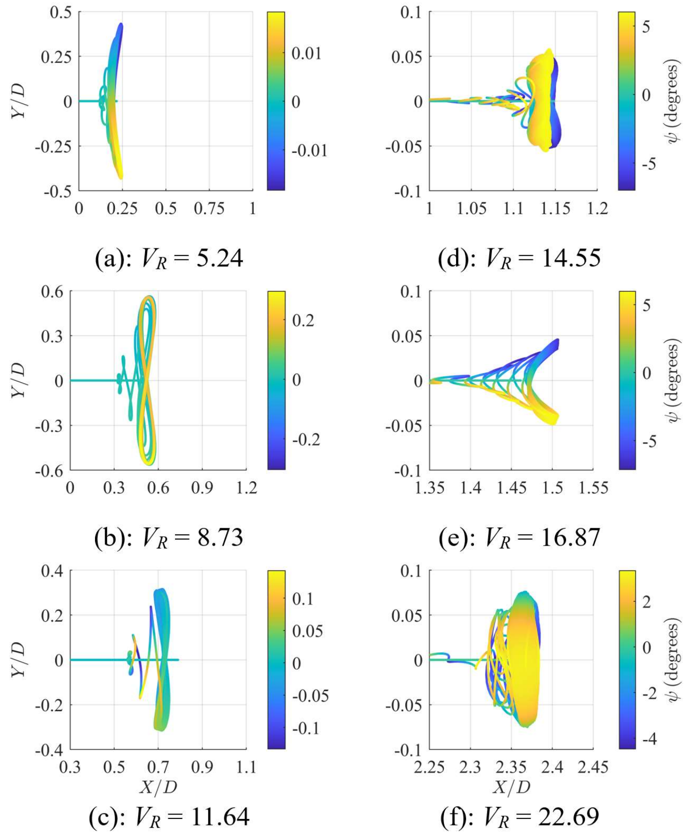

X is the current direction, in-line; Y is the direction transversal to it, cross. Yaw scaled as in the colored bar.

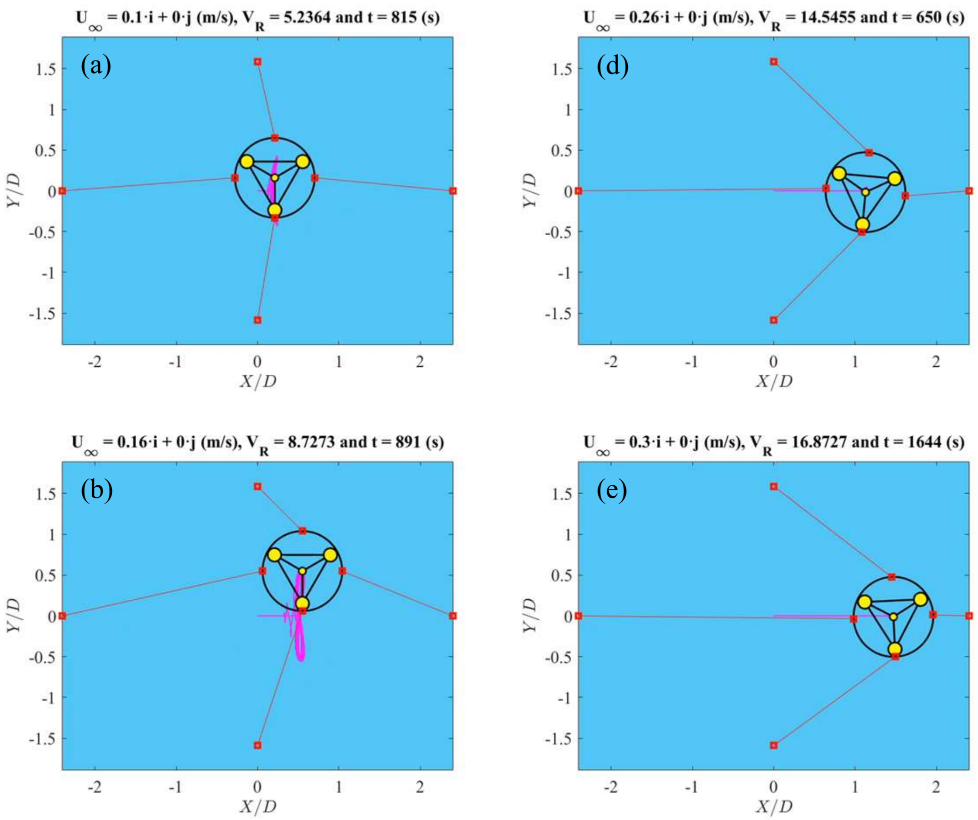

Animation of the FOWT’s motion at the corresponding reduced velocities. Platform drawing in augmented scale (6x).

Results

Trajectories of the FOWT’s center on the horizontal plane

180°

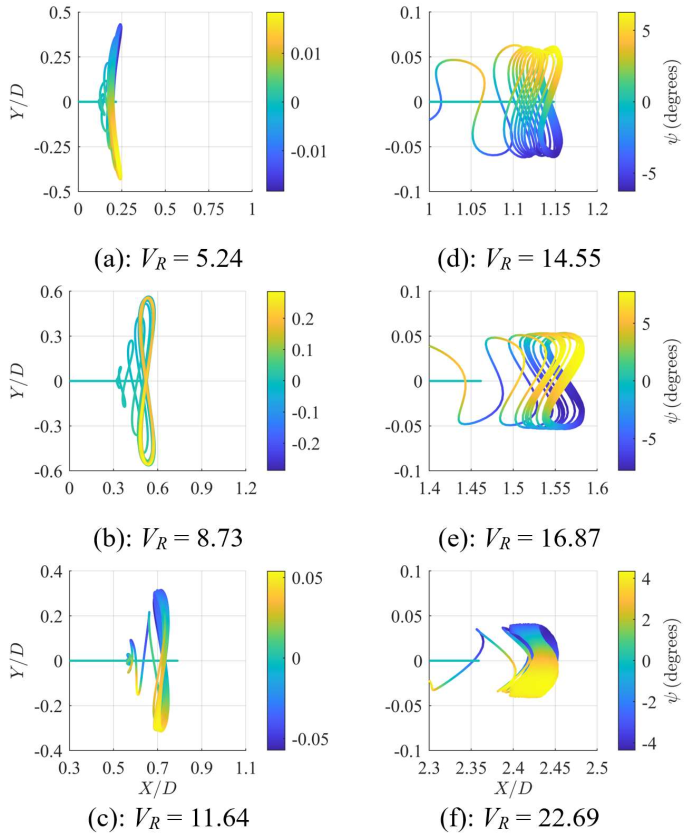

X is the current direction, in-line; Y is the direction transversal to it, cross. Yaw scaled as in the colored bar.

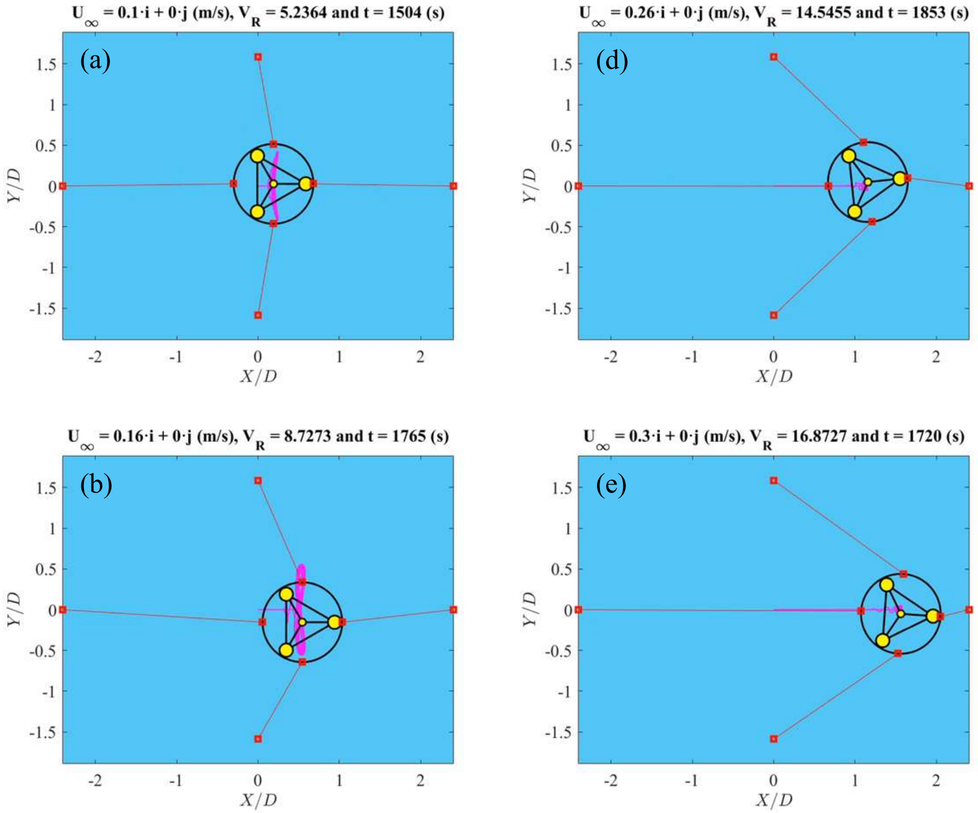

Animation of the FOWT’s motion at the corresponding reduced velocities. Platform drawing in augmented scale (6x).

○ Results

○ Dimensionless amplitudes and frequencies

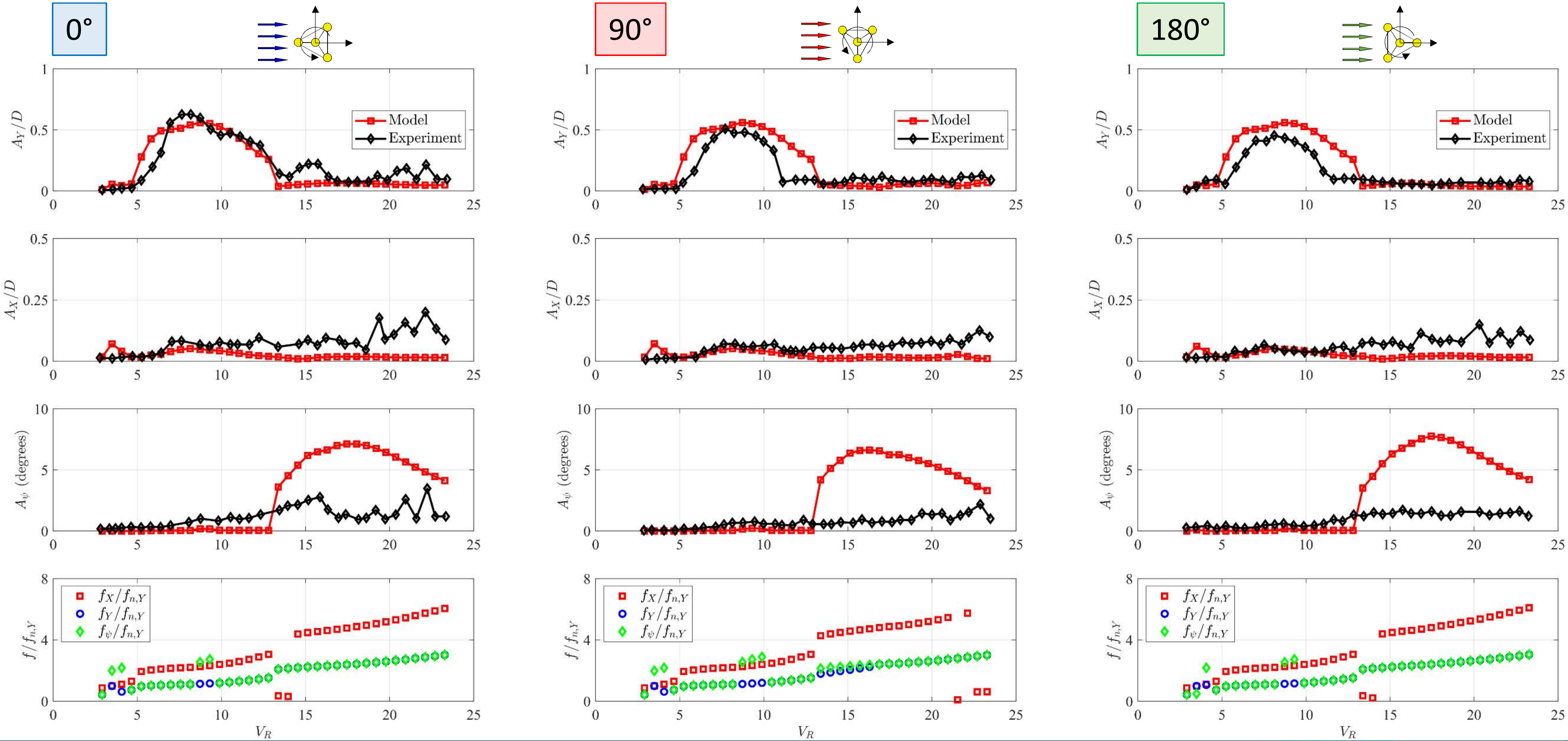

- Numerical Study of a Full-Scale FOWT
  - **FOWT with pontoons**

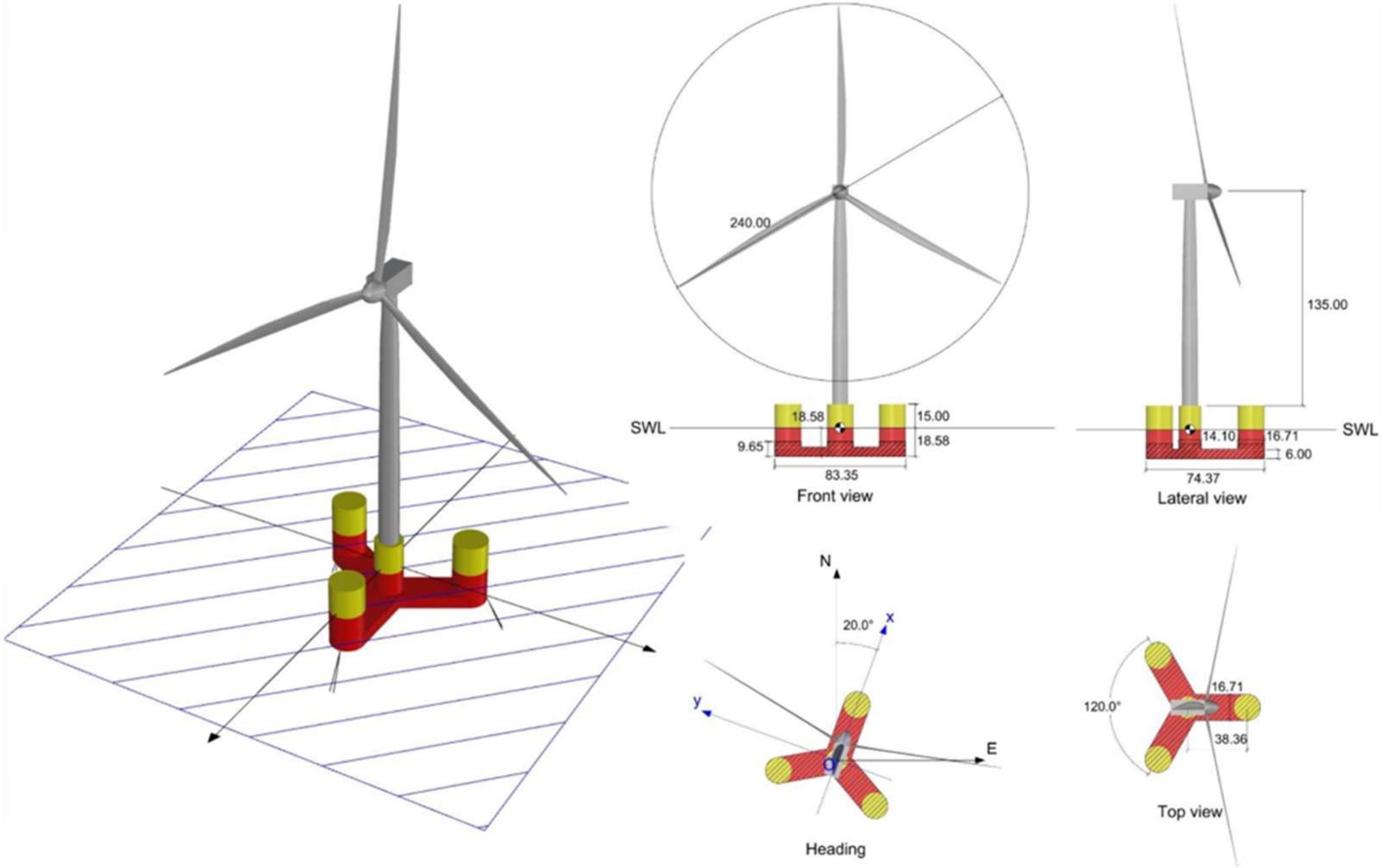

Numerical Study of a Full-Scale FOWT

- **FOWT with pontoons**

The platform is rotated relative to the fixed frame to set up the different heading angles.

$$\hat{\mathbf{M}}_\sigma = \mathbf{R}(\sigma)\hat{\mathbf{M}}_0\mathbf{R}^T(\sigma)$$

$$\hat{\mathbf{K}}_\sigma = \mathbf{R}(\sigma)\hat{\mathbf{K}}_0\mathbf{R}^T(\sigma)$$

0º

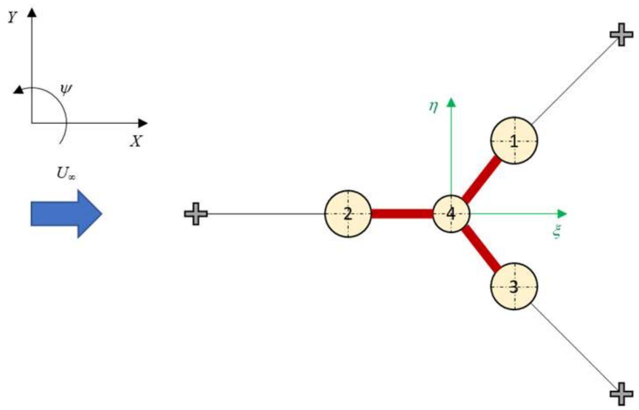

90º

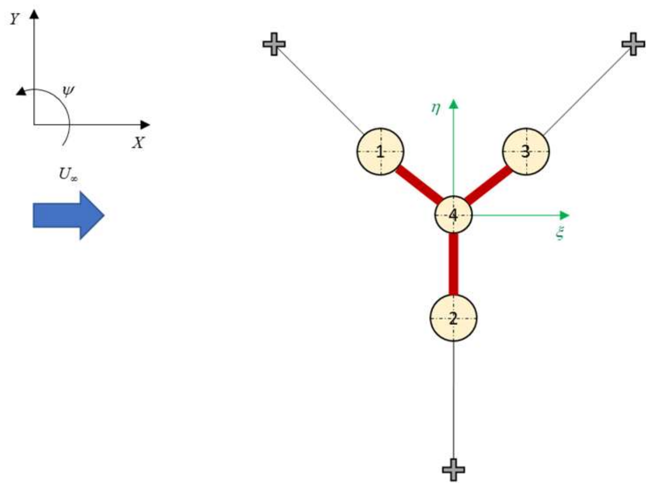

180º

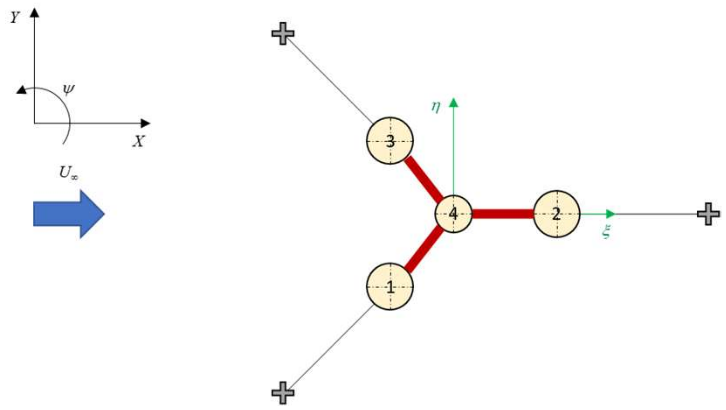

- Numerical Simulations
  - **Simulations' setup**
    - Simulations were carried out at least for 20 reduced velocities ($1 < V_R < 36$ and $1.6 \times 10^6 < Re < 34 \times 10^6$) for each incidence angle;
    - The simulations were performed in a MATLAB® environment, numerically integrating the coupled equations in the state space form;
    - A fixed time step of 0.1 seconds was used, applying the 4th order Runge-Kutta algorithm;
    - The results obtained are:
      1) Natural periods at the trivial equilibrium position (origin, $\boldsymbol{q} = \boldsymbol{0}$);
      2) FOWT's trajectories on the horizontal plane;
      3) Dimensionless motion amplitudes and oscillation frequencies.

- Numerical Simulations
  - **Parameters**

Table 6. FOWT-C parameters.

Parameters	Values	Units
Rigid body mass, $\mathbf{M}_{RB}$	$\begin{bmatrix} 2.25 \cdot 10^7 & 0 & 0 \\ 0 & 2.25 \cdot 10^7 & 0 \\ 0 & 0 & 1.92 \cdot 10^{10} \end{bmatrix}$	kg, kgm^2
Water density, ρ	1025	kg/m^3
Distance between the plataform center and columns centers, R	38.36	m
Columns diameters, D_1, D_2, D_3, D_4	16.71, 16.71, 16.71, 14.1	m
Pontoons dimensions, L, B, H	23, 16.71, 6	m
Strips lengths, Δ_s	2.3	m
Strouhal number of the columns, $S_{t,1}, S_{t,2}, S_{t,3}, S_{t,4}$	0.12, 0.12, 0.12, 0.132	–
Mean drag coefficient of the columns, $C_{D,0}$	0.7	–
Pontoons drag coefficient, C_D	0.61	–

Numerical Simulations

Parameters

Mooring stiffness matrix calculated at the trivial equilibrium position (origin, $\boldsymbol{q} = \mathbf{0}$)

0º

(i) Matriz de massa adicional (kg, kgm, kgm²)

$$\widehat{\mathbf{M}}_A = \begin{bmatrix} 1.45 \cdot 10^7 & 0 & 0 \\ 0 & 1.45 \cdot 10^7 & 1.22 \cdot 10^6 \\ 0 & 1.22 \cdot 10^6 & 1.63 \cdot 10^{10} \end{bmatrix}$$

(ii) Matriz de rigidez (N/m, N/rad, Nm/rad)

$$\widehat{\mathbf{R}} = \begin{bmatrix} 1.65 \cdot 10^4 & 0 & 0 \\ 0 & 1.65 \cdot 10^4 & 2.58 \cdot 10^3 \\ 0 & 2.58 \cdot 10^3 & 2.05 \cdot 10^8 \end{bmatrix}$$

(iii) Frequências naturais (Hz)

$$f_{n,X} = 0.0034;\ f_{n,Y} = 0.0034;\ f_{n,\psi} = 0.0121$$

90º

(i) Matriz de massa adicional (kg, kgm, kgm²)

$$\widehat{\mathbf{M}}_A = \begin{bmatrix} 1.45 \cdot 10^7 & 0 & -1.22 \cdot 10^6 \\ 0 & 1.45 \cdot 10^7 & 0 \\ -1.22 \cdot 10^6 & 0 & 1.63 \cdot 10^{10} \end{bmatrix}$$

(ii) Matriz de rigidez (N/m, N/rad, Nm/rad)

$$\widehat{\mathbf{R}} = \begin{bmatrix} 1.65 \cdot 10^4 & 0 & -2.58 \cdot 10^3 \\ 0 & 1.65 \cdot 10^4 & 0 \\ -2.58 \cdot 10^3 & 0 & 2.05 \cdot 10^8 \end{bmatrix}$$

(iii) Frequências naturais (Hz)

$$f_{n,X} = 0.0034;\ f_{n,Y} = 0.0034;\ f_{n,\psi} = 0.0121$$

180º

(i) Matriz de massa adicional (kg, kgm, kgm²)

$$\widehat{\mathbf{M}}_A = \begin{bmatrix} 1.45 \cdot 10^7 & 0 & 0 \\ 0 & 1.45 \cdot 10^7 & -1.22 \cdot 10^6 \\ 0 & -1.22 \cdot 10^6 & 1.63 \cdot 10^{10} \end{bmatrix}$$

(ii) Matriz de rigidez (N/m, N/rad, Nm/rad)

$$\widehat{\mathbf{R}} = \begin{bmatrix} 1.65 \cdot 10^4 & 0 & 0 \\ 0 & 1.65 \cdot 10^4 & -2.58 \cdot 10^3 \\ 0 & -2.58 \cdot 10^3 & 2.05 \cdot 10^8 \end{bmatrix}$$

(iii) Frequências naturais (Hz)

$$f_{n,X} = 0.0034;\ f_{n,Y} = 0.0034;\ f_{n,\psi} = 0.0121$$

○ Results

○ Trajectories of the FOWT's center on the horizontal plane

0°

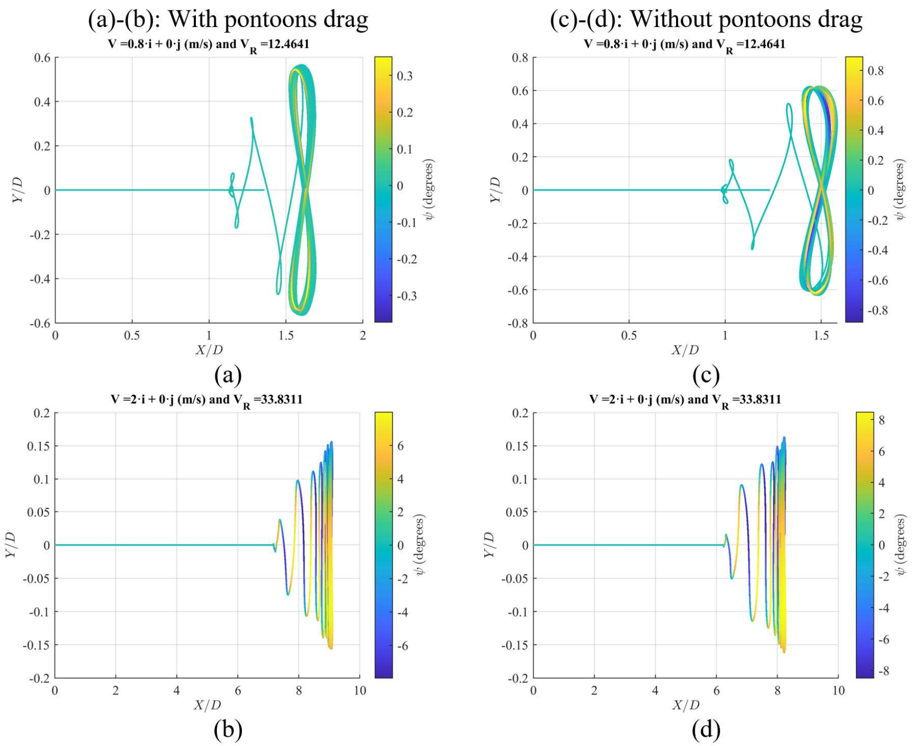

X is the current direction, in-line; Y is the direction transversal to it, cross. Yaw scaled as in the colored bar.

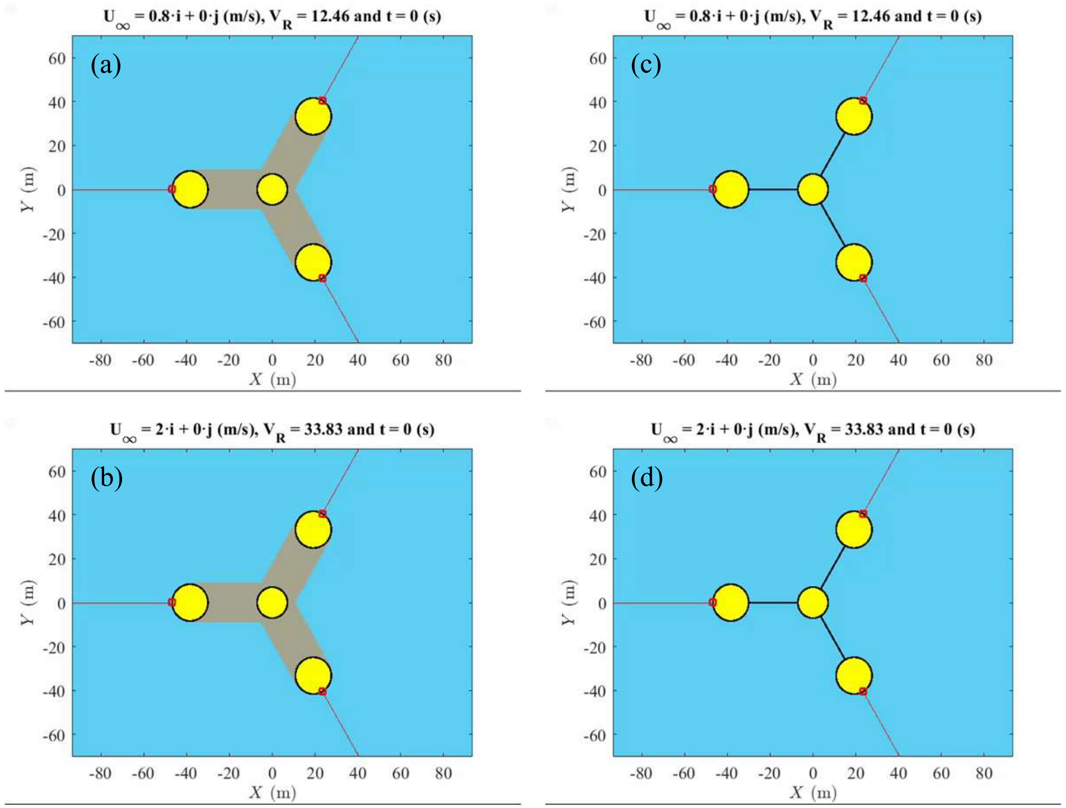

Animation of the FOWT's motion at the corresponding reduced velocities. Platform drawing in augmented scale (3x).

Results

Trajectories of the FOWT's center on the horizontal plane

90°

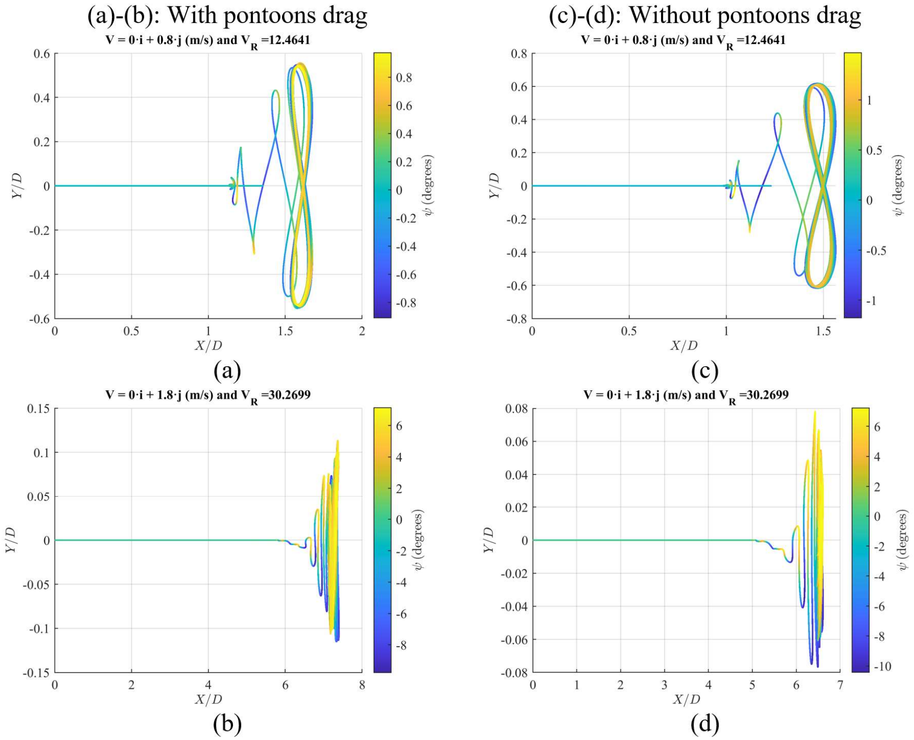

X is the current direction, in-line; Y is the direction transversal to it, cross. Yaw scaled as in the colored bar.

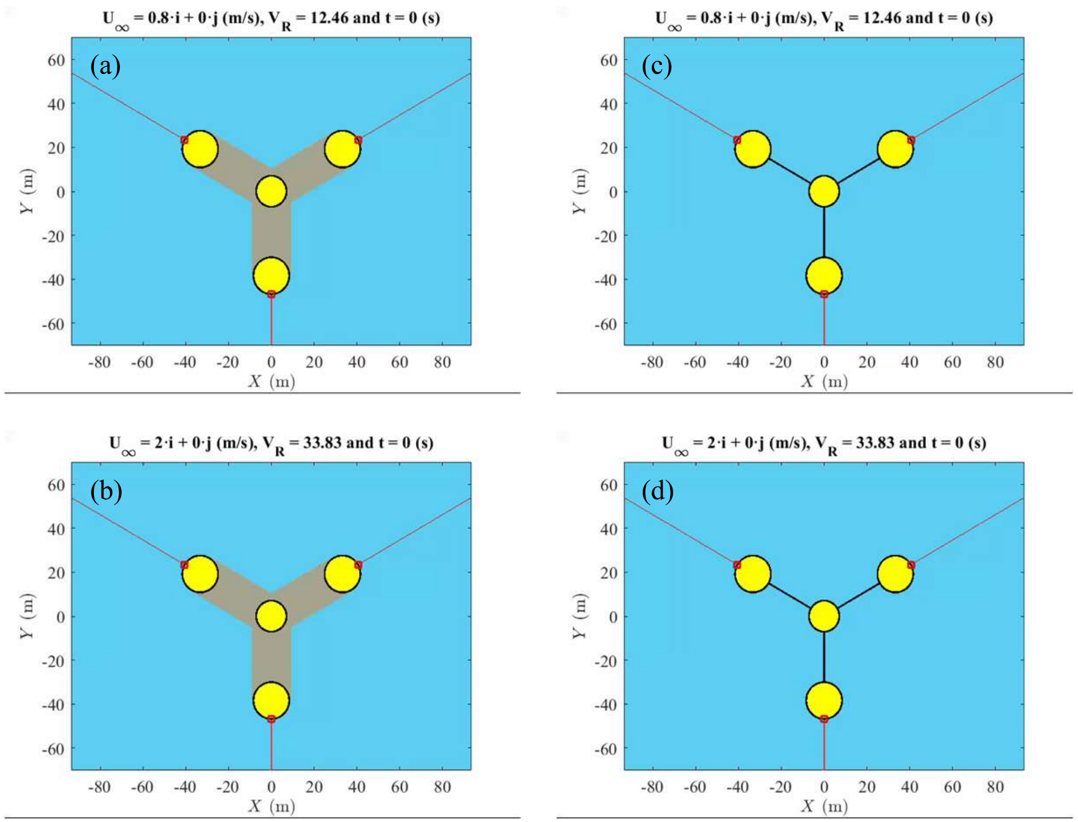

Animation of the FOWT's motion at the corresponding reduced velocities. Platform drawing in augmented scale (3x).

○ Results

○ Trajectories of the FOWT's center on the horizontal plane

180°

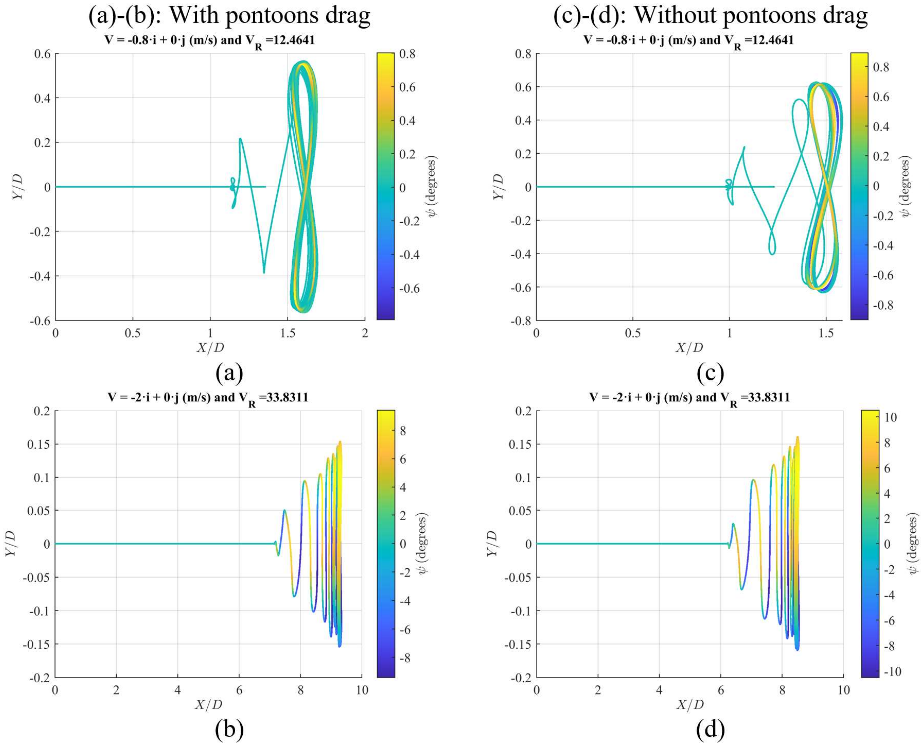

X is the current direction, in-line; Y is the direction transversal to it, cross. Yaw scaled as in the colored bar.

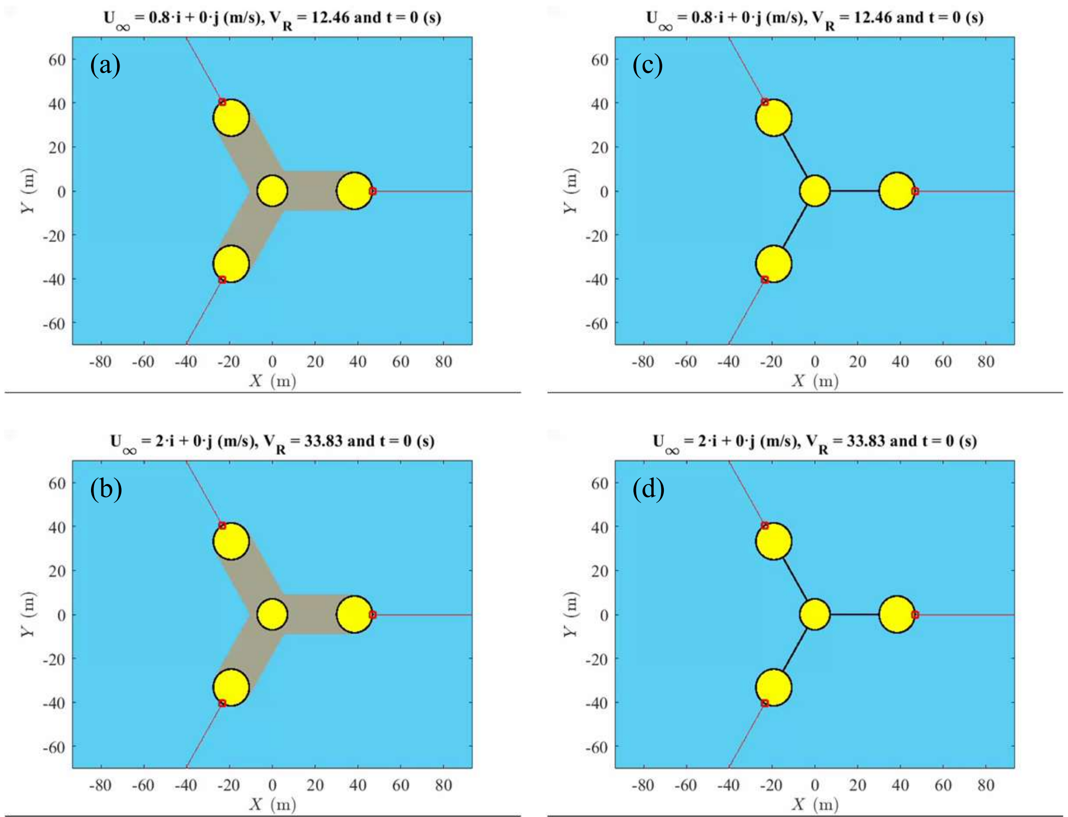

Animation of the FOWT's motion at the corresponding reduced velocities. Platform drawing in augmented scale (3x).

Results

Dimensionless amplitudes and frequencies

0°

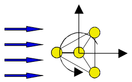

(a)-(b): With pontoons drag

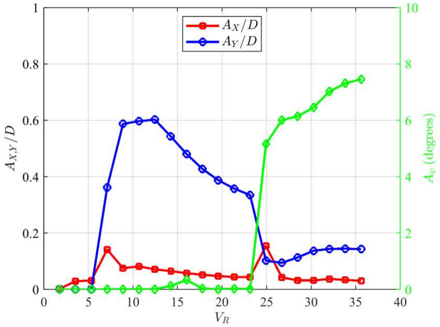

(a)

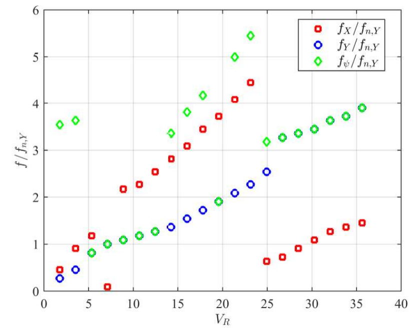

(b)

(c)-(d): Without pontoons drag

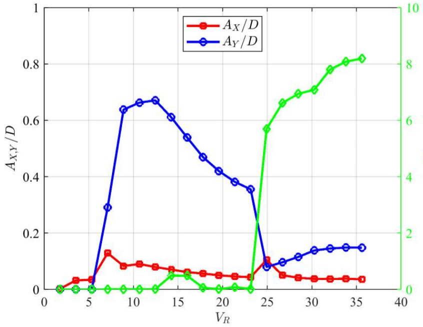

(c)

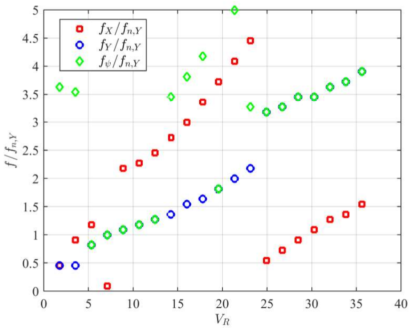

(d)

90°

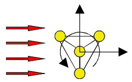

(a)-(b): With pontoons drag

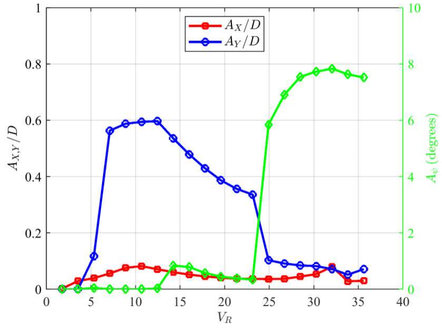

(a)

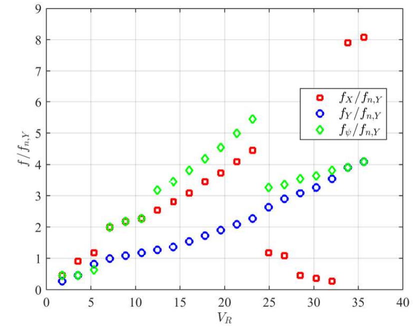

(b)

(c)-(d): Without pontoons drag

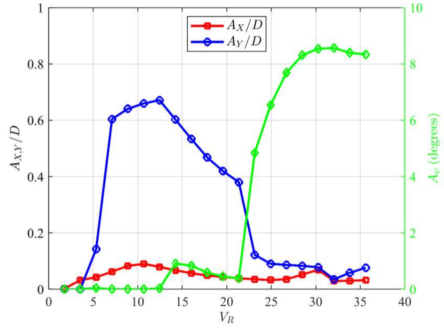

(c)

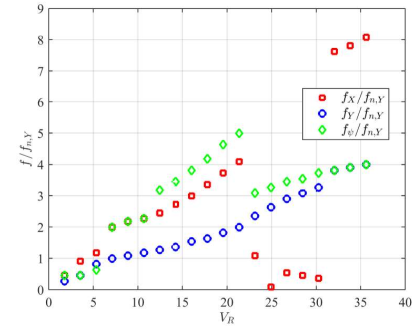

(d)

- Results
  - **Dimensionless amplitudes and frequencies**

180°

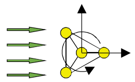

(a)-(b): With pontoons drag

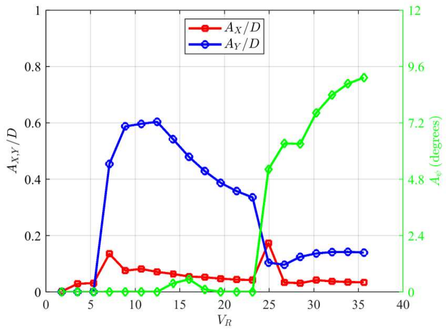

(a)

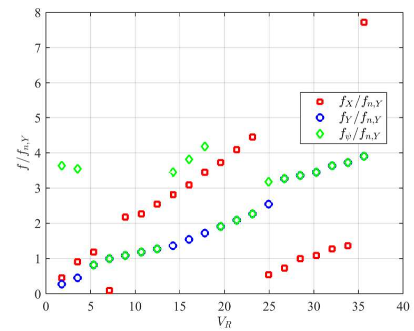

(b)

(c)-(d): Without pontoons drag

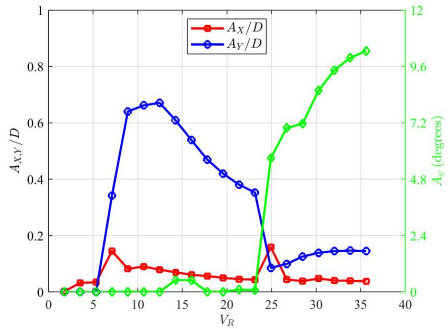

(c)

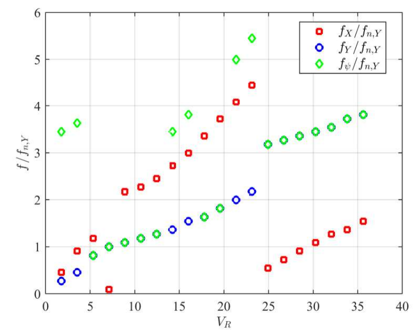

(d)

1) Introduction

2) Motivation and Objectives

3) The Reduced-Order Mathematical Model

4) A Case Study

5) Conclusions and Further Works

6) References

Comments

- A reduced-order mathematical model (ROM) was proposed to address the Vortex-Induced Motion (VIM) of moored (circular) multicolumn FOWTs;
- Viscous fluid forces induced by vortex-shedding are modeled through a phenomenological approach, such that the dynamics of the vortex wake that is shed from each cylindrical column is represented through a pair of wake-oscillators, of the van der Pol type;
- All wake interferences that may occur among columns have been simply ignored in the presented version of this ROM, for simplicity;
- The preliminary results obtained with the proposed ROM turn it into a very promising approach with good experimental comparisons;
- Future improvements should involve the effects of wake interferences between columns, dependent on the spacing between them and thought to be an important issue in some incidence angles and at higher reduced velocities;
- The hydrodynamic effect of the heave plates and braces are other points that certainly deserve further investigation;
- The pontoons additions into the ROM result in damped cross-flow oscillations;
- CFD simulations are on-going tasks: 2D and then 3D.

References

1) WindEurope. Offshore Wind in Europe. Key trends and statistics 2019. Brussels, Belgium: WindEurope, 2020.
2) Fujarra, A.L.C, Rosettti, G.F., Wilde, J., Gonçalves, R.T. State-of-Art on Vortex-Induced Motion: A Comprehensive Survey After More than One Decade of Experimental Investigation. ASME 31st International Conference on Offshore Mechanics and Arctic Engineering, OMAE2012, Rio de Janeiro, 2012.
3) Aranha, J.A.P. Weak three dimensionality of a flow around a slender cylinder: the Ginzburg-Landau equation. Journal of the Brazilian Society of Mechanical Sciences and Engineering, 26, (4): 355-367, 2004.
4) Huerre, P., Monkewitz, P.A. Local and global instabilities in spatially developing flows. Annual Review of Fluid Mechanics, 22: 473-537, 1990.
5) Hartlen, R.T., Currie, I.G. Lift oscillator model of vortex induced vibration. Journal of the Engineering Mechanics, 96 (5): 577-591, 1970.
6) Iwan, W. D. and Blevins, R. D. A model for vortex induced oscillation of structures. Journal of Applied Mechanics, 41: 581-586, 1974.
7) Skop, R.A., Balasubramanian, S. A new twist on an old model for Vortex-Induced Vibration. Journal of Fluids and Structures, 11 (4): 395-412, 1997.
8) Facchinetti, M.L., de Langre, Biolley, F. Coupling of structure and wake oscillators in vortex-induced vibrations. Journal of Fluids and Structures, 19 (2): 123-140, 2004.

References

9) Fujarra, A., Pesce, C.P. Added mass variation and van der pol models applied to vortex-induced vibrations. ASME 2002 International Mechanical Engineering Congress and Exposition, 207-211, New Orleans, 2002.
10) Cunha, L.D., Pesce, C.P., Wanderley, J., Fujarra, A.L.C. The robustness of added mass in VIV models. ASME 25th International Conference on Offshore Mechanics and Arctic Engineering, OMAE2006-92323, Hamburg, June 4-9, 2006.
11) Bernitsas, M.M., Ofuegbe, J., Chen, Jau-Uei, Sun, H. Eigen-Solution for Flow Induced Oscillations (VIV and Galloping) Revealed at the Fluid-Structure Interface. ASME 2019 38th International Conference on Ocean, Offshore and Arctic Engineering. Glasgow, Scotland, UK. June 9–14, 2019.
12) Ogink, R.H.M., Metrikine, A.V. A wake oscillator with frequency dependent coupling for the modeling of vortex-induced vibration. Journal of Sound and Vibration, 329 (26): 5452-5473, 2010.
13) Franzini, G.R., Bunzel, L.O. A numerical investigation on piezoelectric energy harvesting from Vortex-Induced Vibrations with one and two degrees of freedom. Journal of Fluids and Structures, 77: 196-212, 2018.
14) Postnikov, A., Pavlovskaia, E., Wiercigroch, M. 2-dof CFD calibrated wake oscillator model to investigate vortex-induced vibrations. International Journal of Mechanical Sciences 127: 176-190, 2017.
15) Rosetti, G.F., Fujarra, A.L.C., Nishimoto, K., Ferreira, M.D. A phenomenological model for vortex-induced motions of the monocolumn platform and comparison with experiments. ASME 2009 28th International Conference on Ocean, Offshore and Arctic Engineering, 2009.

References

16) Rosetti, G.F., Gonçalves, R.T., Fujarra, A.L.C., Nishimoto, K. Parametric Analysis of a Phenomenological Model for Vortex-Induced Motions of Monocolumn Platforms. Journal of the Brazilian Society of Mechanical Sciences and Engineering, 33 (6): 139-146, 2011.
17) Gonçalves, R.T., Matsumoto, F.T., Malta, E., Rosetti, G.F., Fujarra, A.L.C., Nishimoto, K. Evolution of the MPSO (monocolumn production, storage and offloading system). Marine Systems & Ocean Technology, 6: 45-53, 2010.
18) Pesce, B.A., Lins de Oliveira, E., Pesce, C.P. Vortex Induced Motions of a Moored Monocolumn Platform. Proceedings of the XVIII International Symposium on Dynamic Problems of Mechanics, Buzios, 2019.
19) Gonçalves, R.T., Franzini, G.R., Rosetti, G.F., Meneghini, J.R., Fujarra, A.L.C. Flow around circular cylinders with very low aspect ratio. Journal of Fluids and Structures, 54: 122-141, 2015.
20) Pesce, C.P., Amaral, G.A., Franzini, G.R. Mooring System Stiffness: A general analytical formulation with an application to Floating Offshore Wind Turbines. ASME 2018 1st International Offshore Wind Technical Conference, IOWTC2018, San Francisco, 2018.
21) Gonçalves, R.T., Chame, M.E., Silva, L.S.P., Koop, A., Hirabayashi, S., Suzuki, H. Experimental study on flow-induced motions (FIM) of a floating offshore wind turbine semi-submersible type (OC4 PHASE II FLOATER). Proceedings of the ASME 2019 2nd International Offshore Wind Technical Conference, IOWTC2019, Malta, 2019.

References

22) Slingsby, M.J. Dynamic interaction of subsea pipeline spans due to vortex-induced vibrations. Master's Thesis, TUDelft, 161 p., 2015.

23) Gonçalves, R.T., Private communication with the authors, 2019.

Thank you!

Acknowledgements to

BR PETROBRAS

CAPES

CNPq
Conselho Nacional de Desenvolvimento Científico e Tecnológico

Special acknowledgments

Alexandre N. Simos, Associate Professor of Marine Hydrodynamics, USP;

Rodolfo Gonçalves, Assistant Professor, University of Tokyo;

Décio C. Donha, Associate Professor of Control Engineering, USP.

LMO | Offshore Mechanics Laboratory

Polytechnic School of
University of São Paulo